ELSEVIER

Thermochimica Acta 383 (2002) 153–160

thermochimica acta

www.elsevier.com/locate/tca

Thermogravimetry (TG) applied to the study of the reaction of mercury with platinum–rhodium alloy

E.Y. Ionashiro, F.L. Fertonani*

Instituto de Química, Universidade Estadual Paulista, Araraquara CP 355, São Paulo, CEP 14.800-900, Brazil.

Received 29 May 2001; accepted 10 July 2001

Abstract

Thermogravimetry (TG) energy dispersive X-ray microanalysis (EDX), scanning electron microscopy (SEM), mapping surface, X-ray diffraction (XRD), inductively coupled plasma emission spectroscopy and atomic spectroscopy with cold vapor generation have been used to study the reaction of mercury with platinum–rhodium (Pt–Rh) alloy. The results suggest that, the electrodeposited Hg film reacts with Pt–Rh to form intermetallic compounds of different stability, when heated indicated by at least four weight loss steps. Intermetallic compounds as $PtHg_4$ and $PtHg_2$ was characterized by XRD. These intermetallic compound are the main product presents on the surface of the samples after remotion of the bulk mercury via thermal desorption techniques.

Keywords: Alloy; Rhodium; Mercury; XRD; Intermetallic

1. Introduction

The existence of Hg in the atmosphere and troposphere as pollutant promotes the contamination of many different kinds of materials and make possible a great number of chemical and electrochemical processes. Mercury present on noble metals and their alloys can also invalidate their utilization, for example, as standard mass prototype, electrical contact in electrical and electronic devices due to the new species formed and oxide formation [1–3].

Pt, Rh, Ir and their alloys have many technological applications: as a catalyst in the petroleum cracking industry; as a catalyst supported on alumina [4], on SiC; as a catalyst support in exhaust catalysts source [5]; on SiO_2 and TiO_2 in the automotive exhaust gas oxidation NO to NO_2 and SO_2 to SO_3 [6,7]; as a chemical catalyst material in ammonia oxidation plants [8], and in many other electrical devices [1]; as microelectrodes and ultramicroelectrodes in electrochemistry [9,10]. Mercury interacts easily with these noble metals and with their alloys [3,11–15], which can be an advantage or a disadvantage depending on the application of the resulting material. Thus, as Hg can be present in petroleum as a contaminant, some problems appear mainly due to the formation of solid intermetallic compounds, since they can modify the catalytic properties in petroleum cracking process. On the other hand, Pt, Hg and other metals can be electrodeposited on conductive diamond thin-film surfaces to produce a novel catalytic electrodes, sensors and detectors [1].

Recently, solid reactions of mercury with pure Pt, pure Rh and a Pt–Ir (20 wt.%) alloy, using different techniques were studied [11,16,17]. The results allowed to suggest that the electrodeposited Hg film,

* Corresponding author. Tel.: +55-16-232-2022; fax: +55-16-222-7932.
E-mail address: fertonan@iq.unesp.br (F.L. Fertonani).

0040-6031/02/$ – see front matter
PII: S0040-6031(01)00680-3

when heated, reacts with pure Pt, platinum–rhodium (Pt–Rh) (10 wt.%) and Pt–Ir (20 wt.%) alloy to form products with different stabilities, indicated by more than one weight loss step. These weight loss steps were associated to the bulk Hg remotion, to the desorption of a monolayer of mercury and to the remotion of Hg from a Pt and Pt–Ir alloy solid solution.

In the present work, mercury films were electrodeposited on Pt–Rh (10 wt.%) alloy foils and the mercury was removed by both thermal desorption, as described previously [11,16,17], and by anodic striping. At the end of each step the sample surface was examined by the following techniques: X-ray diffractometry (XRD), scanning electron microscopy (SEM), energy dispersive X-ray microanalysis (EDX), and atomic absorption and emission spectrometry. These techniques allowed to characterize, in details, the nature of the intermetallic phases formed on the surface of these metal–mercury systems.

2. Experimental

The preparation and pre-treatment of the Pt–Rh (10 wt.%) alloy foils, the Hg electrochemical deposition ($E_{\text{deposit}} = -0.35$ V Ag/AgCl/$KNO_{3(\text{sat})}$; $t_{\text{deposit}} =$ 300 s; without stirring; $C_{\text{HG(I)}} = 60 \times 10^{-3}$ mol l^{-1}), the Hg thermal remotion and the chemical analysis of Hg, Rh and Pt in solution were described previously [11,16,17].

TG curves were obtained from 30 to 900 °C, at 5 °C min^{-1}, under a purified N_2 atmosphere flux (150 ml min^{-1}) using a Mettler Thermoanalyser TA-4000 system.

The sample surfaces were examined before and after they had been heated up to different temperatures or after a partial Hg remotion by anodic stripping, using a JEOL JSM-T330A microscope with a NORAN EDX system coupled, and a D-5000 SIEMENS XRD.

The data generated from the XRD studies were treated using a software AFPAR, Complex des Programme, CNRS, France. This program was utilized to determine the lattice parameters of the possible species formed on Pt–Rh foil surface [22]. This method makes use of the experimental interplanar spacings (d-spacing), and data were taken from an original prototype, like $PtHg_4$ or $RhHg_2$ (values of lattice parameters and the respective reflections) [23], both of which were put together to obtain the experimental lattice parameters [16]. The resulting experimental parameters $(a \pm \sigma)$, $(b \pm \sigma)$, $(c \pm \sigma)$ are presented individually in the text and in Table 4, compared with respective prototype parameters.

3. Results and discussion

Fig. 1 shows the TG and DTG curves for quenched Pt–Rh alloy. These curves depict mass losses in four consecutive steps between 30 and 700 °C. The first mass loss from 30 to 170 °C occurs in a very fast process and can be attributed to the loss of bulk mercury electrodeposited and is in agreement with the results already described [11,15,18]. The quantity of mercury lost in this step corresponds to 66.25% of the total electrodeposited mercury. Fig. 2 shows the SEM images of the Pt–Rh alloy covered by the mercury film. Fig. 2a shows the SEM images of the Pt–Rh alloy surface after mercury remotion by heating up to the temperature corresponding to the end of the

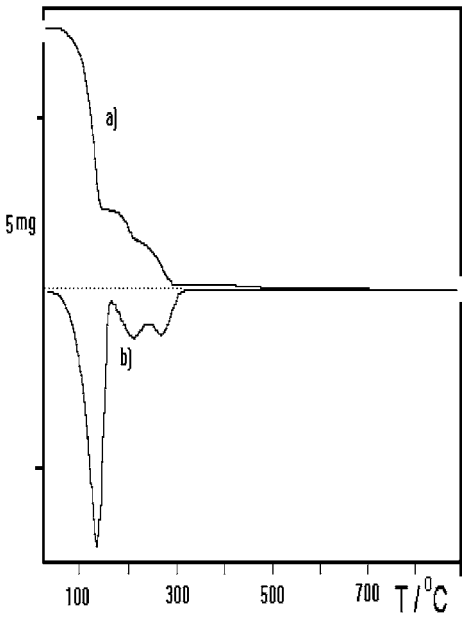

Fig. 1. TG (a) and DTG (b) curves for a quenched Pt–Rh alloy foil containing Hg electrodeposited: heating rate, 5 °C min^{-1}; N_2 flux (purified to remove traces of oxygen), 150 cm^3 min^{-1}.

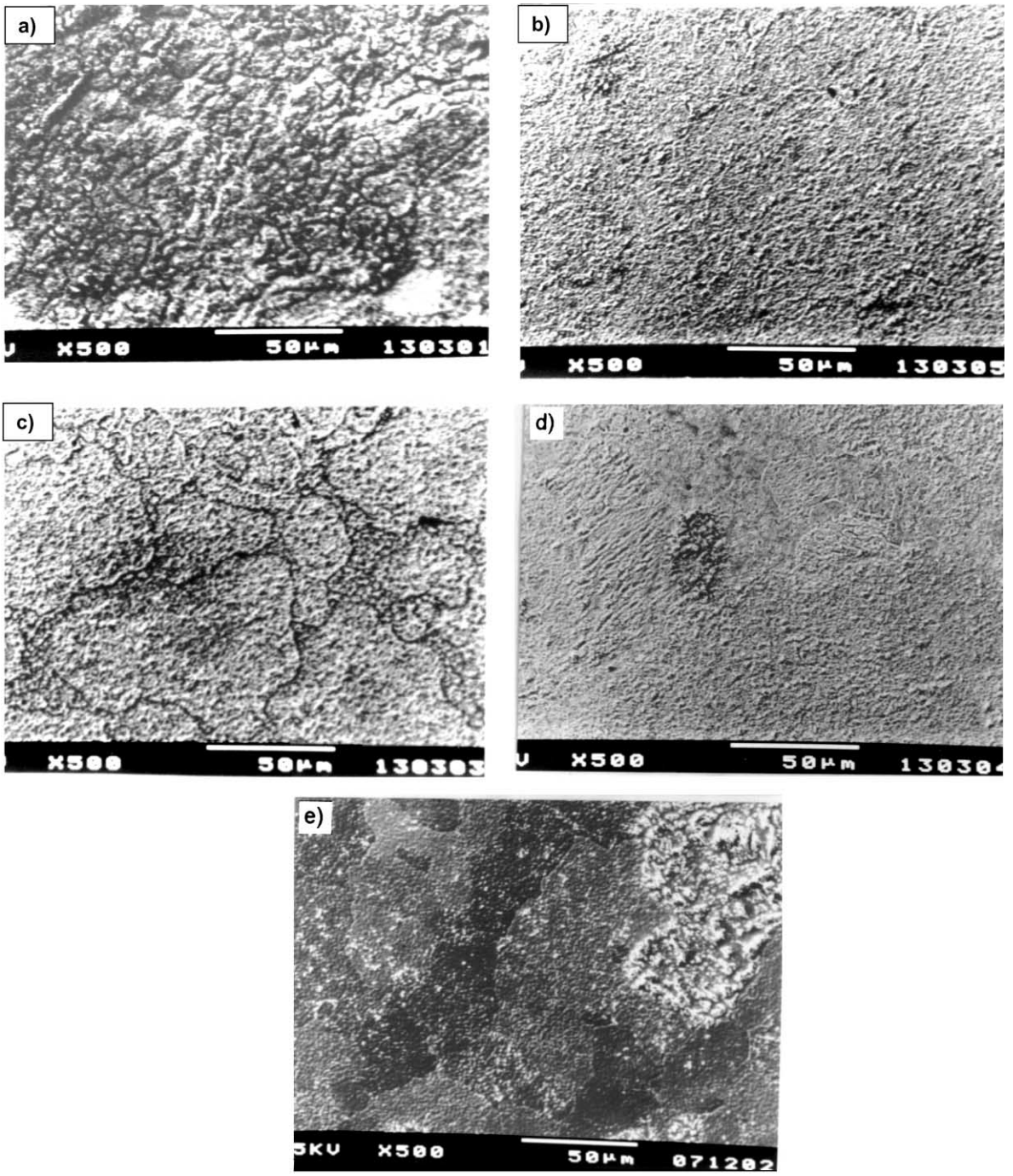

Fig. 2. SEM images of the surface of quenched Pt–Rh alloy after mercury electrodeposition and heated up to: (a) 170 °C; (b) 225 °C; (c) 280 °C; (d) 425 °C; (e) 900 °C.

Table 1
XRD experimental data obtained for the system Pt–Rh–Hg heated up to $T = 180\ ^{\circ}C$; Cu Kα: 1.54184 Å

2θ	Intensity (%)	d_{exp}	d_t	(h k l)	Species
$T = 170\ ^{\circ}C$					
20.30	31	4.375	4.369	(0 1 1)	$PtHg_4$
27.70	7	3.220	3.221	(1 1 0)	$RhHg_2$
28.80	96	3.099	3.090	(0 0 2)	$PtHg_4$
29.70	6	3.008	3.006	(0 0 1)	$RhHg_2$
35.50	14	2.530	2.523	(1 1 2)	$PtHg_4$
41.08	36	2.197	2.198	(1 1 1)	$RhHg_2$
41.20	100	2.190	2.185	(0 2 2)	$PtHg_4$
49.50	81	1.840	1.863	(1 1 3)	$PtHg_4$
51.20	15	1.784	1.784	(2 2 2)	$PtHg_4$
55.50	5	1.670	1.650	(1 2 3)	$PtHg_4$
57.50	6	1.603	1.611	(2 2 0)	$RhHg_2$
59.80	12	1.553	1.545	(0 0 4)	$PtHg_4$
65.30	5	1.429	1.427	(0 1 2)	$RhHg_2$
67.70	9	1.380	1.381	(0 2 4)	$PtHg_4$
69.00	4	1.361	1.362	(1 1 2)	$RhHg_2$

first mass loss step in TG curve. The SEM images show a surface covered by a gray solid film and considerably rough. When a Pt foil with mercury electrodeposited was heated up to 110 °C, at 5 °C min^{-1}, and then cooled to room temperature, a gray solid material, characteristic of the $PtHg_4$ was observed and in agreement with [19]. While the mercury remains on the foil which is being heated up to 110 °C, the Pt solubility increases in the bulk mercury (0.202 at.% at 70 °C to 0.910 at.% at 110 °C) [12]. For this surface the XRD results are presented in Tables 1 and 4 indicating that $PtHg_4$ (cubic system: $a = (6.17 \pm 0.01)$ Å) and $RhHg_2$ (tetragonal system: $a = (4.527 \pm 0.004)$ Å and $b = (2.934 \pm 0.004)$ Å) are the most probable species formed on the foil.

The second and third steps observed between 170–225 °C and 225–280 °C, as ascribed to the remotion of the mercury initially contained in the $PtHg_4$ film, as already observed in other works described in [15,17,18,20]. For temperatures ranging from 170 to 280 °C the mass loss was 13.8 and 17.6% of the total mercury electrodeposited for the second and third steps, respectively. The existence of mercury on the Pt–Rh alloy surface at the end of these steps were confirmed by EDX microanalysis (Fig. 3) and atomic absorption spectrometry (Table 3). $PtHg_2$ (tetragonal system: $a = (4.666 \pm 0.005)$ Å and $b = (2.913 \pm 0.003)$ Å) and $RhHg_2$ (Tables 2 and 4) were also identified by XRD at the end of the second step.

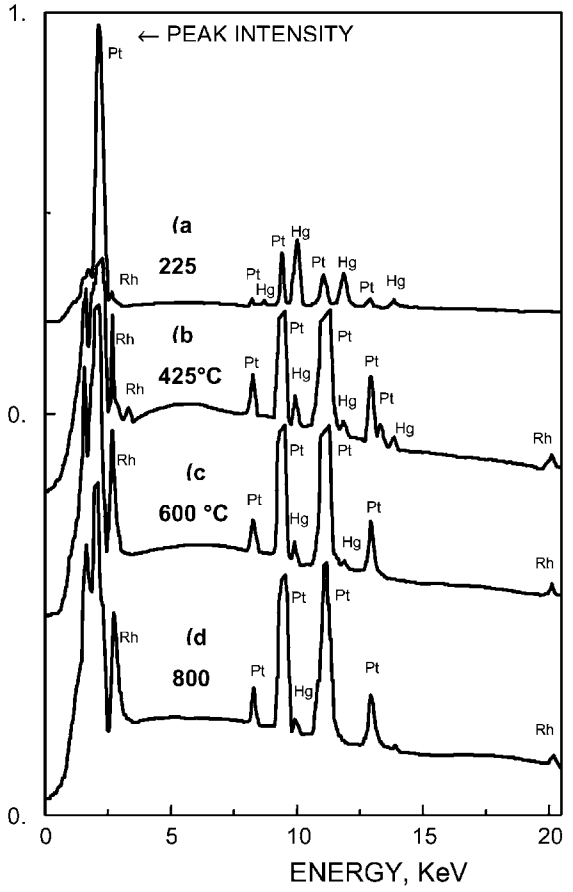

Fig. 3. EDX microanalysis of the surface of quenched Pt–Rh alloy heated up to different temperatures. Sample time: (a) 100 s; (b) and (c) 300 s; (d) 500 s. Electron beam acceleration: 30 kV.

For atomic emission analysis the Pt–Rh foil surfaces heated up to 170 °C were attacked as already described [11]. It is interesting to note that in the present study, platinum and rhodium were also detected in the resulting solution like in Pt–Ir system (Table 3). These results putting in evidence the surface instability of the Pt–Rh alloy caused by its interaction with mercury. This seems to indicate that the atomic size factor between Hg and Rh and Pt introduces a surface destructuration, which facilitates the attack of the surface by the acid solution [11,16].

The SEM images of the alloy surface after partial mercury remotion by heating up to temperatures corresponding to the final of the second and the third

Table 2
XRD experimental data obtained for the system Pt–Rh–Hg heated up to $T = 225$, 280 and 425 °C; Cu Kα: 1.54184 Å

2θ	Intensity (%)	d_{exp}	d_t	(h k l)	Species
$T = 225$ °C					
35.80	12	2.508	2.509	(0 1 1)	$RhHg_2$
36.22	48	2.480	2.476	(0 1 1)	$PtHg_2$
38.65	100	2.329	2.337	(0 2 0)	$PtHg_2$
39.33	24	2.291	2.280	(1 1 0)	Pt_3O_4
39.55	20	2.278	2.278	(0 2 0)	$RhHg_2$
39.72	13	2.267	2.266	(1 2 1)	Rh_2O_3
43.20	19	2.094	2.091	(1 2 0)	$PtHg_2$
45.45	11	1.996	1.993	(1 2 2)	Rh_2O_3
45.72	27	1.984	1.975	(0 2 2)	Pt_3O_4
68.20	49	1.375	1.375	(0 3 1)	$PtHg_2$
69.50	22	1.353	1.355	(0 3 1)	$RhHg_2$
$T = 280$ °C					
38.80	20	2.321	2.329	(2 1 0)	$PtHg_2$
39.45	67	2.284	2.280	(1 1 2)	Pt_3O_4
39.70	77	2.267	2.266	(1 2 1)	Rh_2O_3
41.55	14	2.173	2.184	(1 0 3)	Rh_2O_3
44.95	15	2.017	2.023	(1 1 3)	Rh_2O_3
46.15	44	1.967	1.975	(0 2 2)	Pt_3O_4
67.43	11	1.388	1.387	(1 3 3)	Rh_2O_3
$T = 425$ °C					
27.70	18	3.220	3.223	(1 1 0)	$PtHg_2$
39.25	17	2.298	2.280	(1 1 2)	Pt_3O_4
39.80	100	2.265	2.266	(1 2 1)	Rh_2O_3
41.40	14	2.181	2.187	(1 0 3)	Rh_2O_3
44.52	12	2.035	2.038	(1 2 0)	$PtHg_2$
46.25	54	1.963	1.959	(2 1 2)	Rh_2O_3
67.50	13	1.388	1.387	(0 1 2)	Rh_2O_3

steps of the TG curve are show in Fig. 2b and c. The greater partial remotion of mercury shows a well defined grains boundaries, as pointed out in Fig. 2c, showing that the surface structure was basically maintained, suggesting that the mercury film still exist on the surface. However, the Pt–Rh alloy exhibits a morphology which is very different from that one showed by pure Pt and Pt–Ir alloy [11]. The XRD data obtained at the end of the second step (280 °C) allowed to suggest the existence of $PtHg_2$ species (Tables 2 and 4). It was also observed a series of peaks in the X-ray pattern which were attributed to oxide formation (Pt_3O_4-cubic system and Rh_2O_3-orthorhombic system). The signals corresponding to $PtHg_2$ species disappear as the heating temperature increases.

The second step of TG–DTG curves can be attributed to the existence of the $RhHg_2$ species in the matrix of the $PtHg_4$, forming a solid solution which changes the conditions of the diffusion of the heat and consequently diminishes the reaction rate. The reduction of this reaction rate promotes the appearing of the third step in the TG curve. Therefore, it is possible to suggest the following solid reactions:

$$\text{second step}: \quad PtHg_4 \rightarrow PtHg_2 + 2Hg \quad (13.8\%) \tag{1}$$

$$\text{third step}: \quad PtHg_2 \rightarrow Pt + 2Hg \quad (17.4\%) \tag{2}$$

and that both, $RhHg_2$ and $PtHg_2$, decomposed together in the third step. The difference in the mass loss percentage (3.6%), between reactions (1) and (2), cannot be attributed only to the decomposition of $RhHg_2$. It is important to note the presence of $PtHg_2$ at the end of the third step (280 °C), and the disappearance of the signals corresponding to the $PtHg_2$ species in the X-ray pattern when the sample is heated from 280 to 600 °C. These observations suggest the presence of a PtHg film. This film, in a first moment, was possibly present under the film of $PtHg_4$–$RhHg_2$ solid solution and undergoes an eutectoide dispropor-

Table 3
Atomic absorption flameless and atomic emission (AES–ICP) data for Hg, Pt and Rh after partial or total elimination of the mercury heated up to the temperatures specified

Material	T (°C)	m_i[a] (mg)	m(Hg) (mg)	m(Pt) (mg)	m(Rh) (mg)
Pt–Rh (quenched)	25	14.721	1.76	1.11	0.0649
	180	11.730	1.47	0.700	0.0417
	230	9.110	0.313	0.450	0.0229
	280	9.479	0.0162	0.670	0.0339
	600	9.906	0.00428	0.248	0.00659
	800	21.517	0.00160	0.00704	0.00347

[a] m_i: total initial mass.

Table 4
Comparison between calculated crystalline lattice parameters, using the experimental data from Tables 1 and 2, with theoretical prototype parameters [22,23]

Prototype lattice parameters [23]	Experimental lattice parameters[a]		Difference (%)
	$(a \pm \sigma)$ Å	$(c \pm \sigma)$ Å	
Thermal analysis			
$T = 170$ °C, $PtHg_4$; $a = 6.181$ Å	6.17 ± 0.01	–	0.07
$T = 225$ °C, $PtHg_2$; $a = 4.675$ Å; $c = 2.918$ Å	4.667 ± 0.004	2.913 ± 0.004	*a*: 0.50; *b*: 0.20
$T = 225$ °C, $RhHg_2$; $a = 4.557$ Å; $c = 3.003$ Å	4.527 ± 0.003	2.934 ± 0.004	*a*: 0.70; *b*: 2.3

[a] Calculated using software from [22].

tionation [21] producing a $PtHg_2$ species and a solid solution according to the reaction

$$PtHg \rightarrow PtHg_2 + Pt(Hg) \quad (3)$$

The $PtHg_2$ intermetallic compound was identified by XRD at the sample surface heated up to temperatures corresponding to the end of the third mass loss step in the TG curve (Fig. 1). It is also known that in a temperature ranging from 230 to 300 °C, the solubility of Hg in Pt increases (0.2 at.% at 200 °C to 16.1 at% at 300 °C) [12].

The formation of $PtHg_2$ at the end of the third step (reaction (3)) was also verified in a experiment carried out using pure Pt as substrate containing only $PtHg_4$ on the surface of the foil. In this experiment, the bulk mercury was removed previously maintaining the foil under an isotherm for 10 min at 120 °C. The TG curve obtained immediately after the bulk mercury remotion showed mass loss in two steps (Fig. 4). The first step, a very fast process which corresponds to the conversion of $PtHg_4$ (confirmed by XRD) to $Hg_{(g)}$ and Pt, and for the second step a slow process, corresponding to 5% of the total mass loss, which can be attributed to the decomposition of the $PtHg_2$ formed according to the reaction (3). $PtHg_2$ was determined on the foil surface of pure platinum at the temperature of 230 °C using XRD.

The remotion of the mercury electrodeposited on the Pt–Rh alloy surface occurs in four steps, while for the Pt and Pt–$Ir_{(20\%)}$ alloy the remotion occurs in three steps [11,16,17]. The disagreement is observed after the remotion of the bulk mercury, where in the Pt–Rh alloy the presence of $RhHg_2$ stabilize the intermediate $PtHg_2$ formed during the thermal decomposition of the $PtHg_4$. Therefore, for the Pt–Rh alloy two steps are observed between 160 and 280 °C.

The last mass loss step for the Pt–Rh alloy system corresponds to a very slow process and can be related to the mercury remotion from a solid solution as previously suggested [11,18]. Affrosman and co-workers [15,18] observed a complete mercury remotion from pure platinum when the sample was heated at temperatures until approximately 500 °C, while

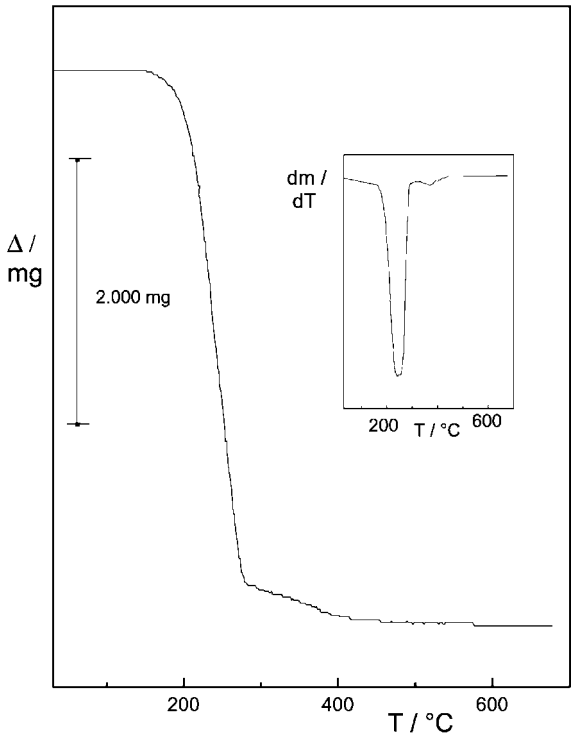

Fig. 4. TG (a) and DTG (b) curves for pure Pt foil containing PtHg intermetallic compounds: heating rate, 5 °C min^{-1}; N_2 flux (purified to remove traces of oxygen), 150 cm^3 min^{-1}. Remark: bulk mercury was previously removed maintaining the foil under an isotherm for 10 min at 120 °C.

Fertonani et al. [11] had detected mercury on the foil surface even at temperatures around of 600 °C, and until approximately 800 °C to Pt–Ir alloys. In this step, the mass loss was 1.7% to pure platinum and 1.2% to Pt–Ir alloy. On the other hand, for Pt–Rh alloy, 2% of the total electrodeposited mercury was detected after the sample had been heated up to 700 °C. Mercury was also detected on foil surfaces (Pt–Rh) by EDX (Fig. 3c when the samples were heated up to 600 °C. These results agree with that obtained using atomic emission analysis (Table 3). For Pt–Rh alloy, the intensity of the Hg peaks diminishes in EDX microanalysis as the heating temperature increases. To pure Pt, mercury has not been detected at heating temperatures higher than 800 °C while mercury still exists on the Pt–Rh and Pt–Ir alloy surfaces at that temperature.

The Fig. 2d and e show the SEM images of the Pt–Rh alloy surface after mercury remotion by heating up to 425 and 900 °C, temperatures corresponding to the middle and to the end of the last mass loss step in TG curves, respectively. At this step the mercury existent in the amalgam was slowly removed and the surface was not rearranged, comparing to Pt and Pt–Ir (20 wt.%) systems, at 900 °C [11]. Differently from SEM images obtained for Pt and Pt–Ir systems, at the same range of temperature, Pt–Rh alloy surface exhibits not only a considerable roughening but also the grain boundaries are not so clearly observed. The X-ray pattern obtained for samples heated at 425 °C is shown in Table 2. These data had indicated $PtHg_2$ as a principal compound formed on the Pt–Rh foil surface at this temperature (according to reaction (3)) and the presence of other peaks that correspond to metal oxides like Rh_2O_3 and Pt_3O_4.

When the heating temperature was increased to 600 °C, $PtHg_2$ peaks disappear and only oxides and substrate peaks were observed in XRD. However, mercury was also detected on the foil surface at the same temperature range by EDX microanalysis (Fig. 3c–e), showing the amalgam formation. The existence of mercury in the lattice was also confirmed by atomic emission analysis (Table 3).

4. Conclusion

The studies presented here allowed to characterize the mercury film formed on Pt–Rh (10 wt.%) alloy surface and also suggested intermetallic compound formation on the alloy surface and the amalgam formation in its subsurface. The film is formed by mercury electrodeposition on metal alloy foils followed by a reaction of mercury with the alloy surface probably assisted by heating at different temperatures.

The system Pt–Rh–Hg loses mercury in at least four steps: from the room temperature to 170 °C, only the bulk Hg was removed, and a solid solution $PtHg_4$ and $RhHg_2$ film was found covering a possible thick film of PtHg; between 170 and 225 °C, the second mass loss was attributed to the thermal decomposition of the $PtHg_4$ compound, generating $Hg_{(g)}$ and $PtHg_2$ as an intermediate; the third step, from 225 to 280 °C, was ascribed to the decomposition of the $PtHg_2$ simultaneously whit the $RhHg_2$ species. The last mass loss step, 280–800 °C, was ascribed to the $PtHg_2$ decomposition, formed at 280 °C as a product of the eutectoide disproportionation reaction of PtHg species, and mercury remotion from the PtHg solid solution. The formation of this solid solution cause a great surface instability, ascribed to the atomic size factor between Hg and Rh and Pt, facilitating acid solutions attack on the surface.

EDX microanalysis have proved the presence of mercury on the grain surface and grain boundary after heating up to different temperatures, in agreement with the findings from the TG–DTG curves. The SEM images demonstrate that the grain boundaries and grain surfaces were attacked under specified conditions, possible because mercury have a lower contact angle (Hg-subtract) and completely wet the foil surface. The SEM images obtained at 800 °C for Pt–Rh (10 wt.%) foil reveals a considerably roughening, which was also observed for pure Rh [16], but was absent for pure Pt [17] and Pt–Ir (20 wt.%) alloy [11,17].

References

[1] M. Awada, J. Strojek, G.M. Swain, J. Electrochem. Soc. 142 (1995) L42.
[2] K.G. Kreider, M.J. Tarlov, J.P. Cline, Sensor Actuat. B: Chem. 28 (1995) 165.
[3] P.J. Cumpson, M.P. Seah, Internal Communication, National Physical Laboratory, UK, 1994, p. 32.
[4] R.W. Joyner, E.S. Shpiro, Catal. Lett. 9 (1991) 239.
[5] M.B. Kizling, P. Stenius, S. Andersson, A. Frestad, Appl. Catal. B: Environ. 1 (1992) 149.

[6] E. Xue, K. Seshan, J.G. Vanommen, J.R.H. Ross, Appl. Catal. B: Environ. 2 (1993) 183.
[7] G.E. Poirier, B.K. Hance, J.M. White, J. Phys. Chem. 97 (1993) 5965.
[8] J.L.G. Fierro, J.M. Palacios, F. Tomas, J. Mater. Sci. 27 (1992) 685.
[9] M. Fleishmann, S. Pons, D. Robson, P.P. Schmidt (Eds.), Ultramicroelectrodes, Datatech Science Morganton, NC, 1987.
[10] R.M. Whigtmann, D.O. Wipf, in: A.J. Bard (Eds.), Electroanalytical Chemistry, Vol. 15, Marcel Dekker, New York, 1989.
[11] F.L. Fertonani, A.V. Benedetti, M. Ionashiro, Thermochim. Acta 265 (1995) 151.
[12] C. Guminski, Bull. Alloy Phase Diagrams 11 (1990) 22.
[13] T.B. Massalski, H. Okamoto, P.R. Subramanian, L. Kacprzak (Eds.), Binary Alloy Phase Diagrams, Vol. 3, ASM International Press, USA, 1990.
[14] S.P. Kounaves, J. Buffle, J. Electroanal. Chem. 216 (1987) 53.
[15] S. Affrossman, W.G. Erskine, Trans. Faraday Soc. 62 (1966) 2922.
[16] E. Milaré, F.L. Fertonani, M. Ionashiro, A.V. Benedetti, J. Thermal Anal. Cal. 59 (2000) 617.
[17] F.L. Fertonani, A.V. Benedetti, J. Servant, J. Portillo, F. Sanz, Thin Solid Films 341 (1999) 1.
[18] S. Affrossman, W.G. Erskine, J. Paton, Trans. Faraday Soc. 64 (1968) 2856.
[19] S.K. Lahiri, D. Gupta, J. Appl. Phys. 51 (1980) 5555.
[20] G.D. Robins, C.G. Enke, J. Electroanal. Chem. 23 (1969) 343.
[21] G. Jangg, T. Dortbudak, Z. Metallkd. 64 (1973) 715.
[22] Complex des Programme, CNRS, France, 1990.
[23] Powder Diffraction File PDF2, Data Base Sets 1–44, Jointer Commitee on Powder Diffraction Standard, International Center for Diffraction Data, Pensylvania, 1988 (CD-ROM).